

***Electronic Supplementary Information***

**Structure and magnetic properties of novel heteroheptanuclear metal  
string complex  $[\text{Ni}_3\text{Ru}_2\text{Ni}_2(\mu_7\text{-teptra})_4(\text{NCS})_2](\text{PF}_6)$**

Cheng-Chang Chiu,<sup>a</sup> Ming-Chuan Cheng,<sup>b</sup> Sheng-Hsiang Lin,<sup>a</sup> Cheng-Wei Yan,<sup>a</sup> Gene-  
Hsiang Lee,<sup>a</sup> Mu-Chieh Chang,<sup>\*a</sup> Tien-Sung Lin<sup>\*a</sup> and Shie-Ming Peng<sup>\*a,b</sup>

---

[a] Department of Chemistry, National Taiwan University, No. 1, Sec. 4,  
Roosevelt Rd., 10617 Taipei, Taiwan

E-mail : [smpeng@ntu.edu.tw](mailto:smpeng@ntu.edu.tw); [lin@wustl.edu](mailto:lin@wustl.edu); [mcchang1005@ntu.edu.tw](mailto:mcchang1005@ntu.edu.tw)

[b] Institute of Chemistry, Academia Sinica, 128 Academia Road, Section 2, Nankang,  
Taipei, Taiwan

## **Content**

1. Mass spectrometry for HMSC 1.

**Fig. S1**

2. NMR measurements for HMSC 1.

**Fig. S2**

3. Infrared spectra of HMSC 1.

**Fig. S3**

4. Crystal structural data for HMSC 1.

**Table S1**

5. The EPR spectra and spectral simulation at 20 and 60 K.

**Fig. S4 and Table S2**

## 1. Mass spectra of HMSC 1.

MALDI-mass spectra of HMSC 1 were obtained with a Bruker, New ultrafleXtreme™. The peaks show that the distributions of experimental results are consistent with the simulation data for the target complex.

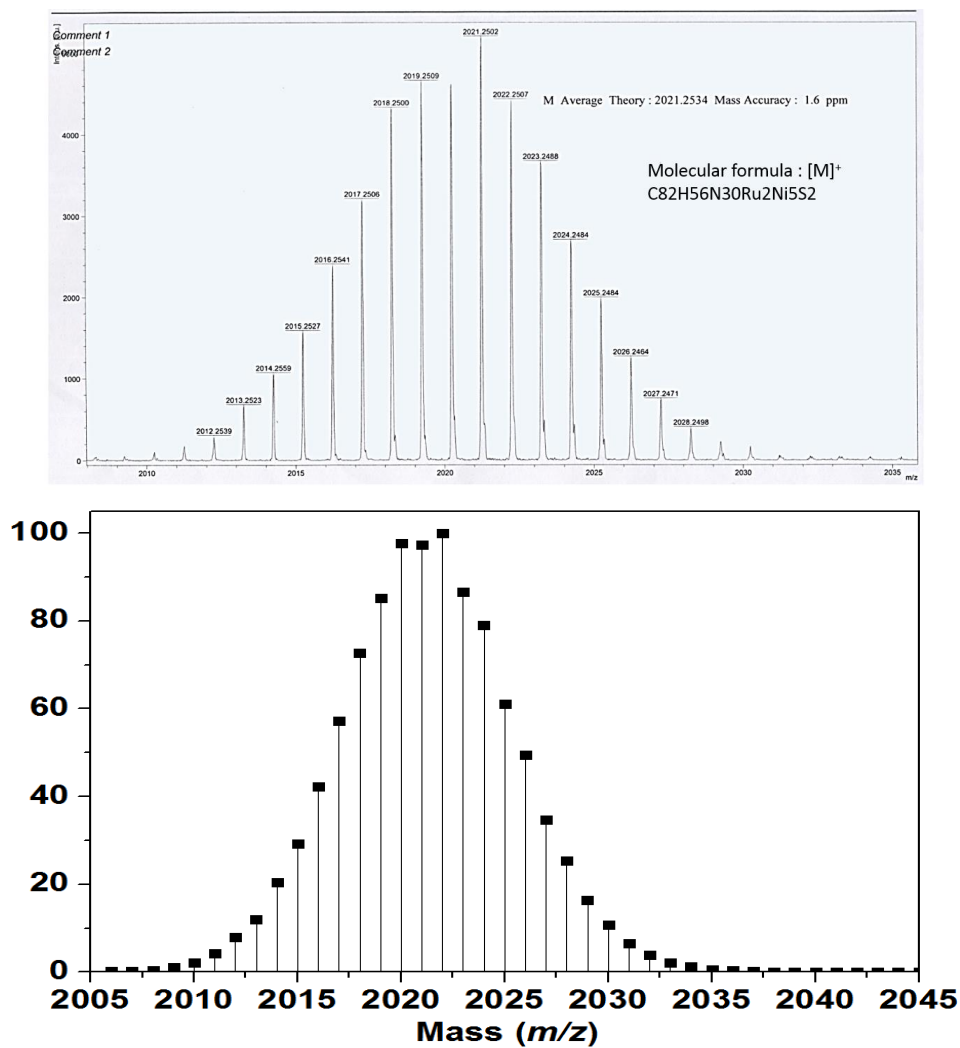
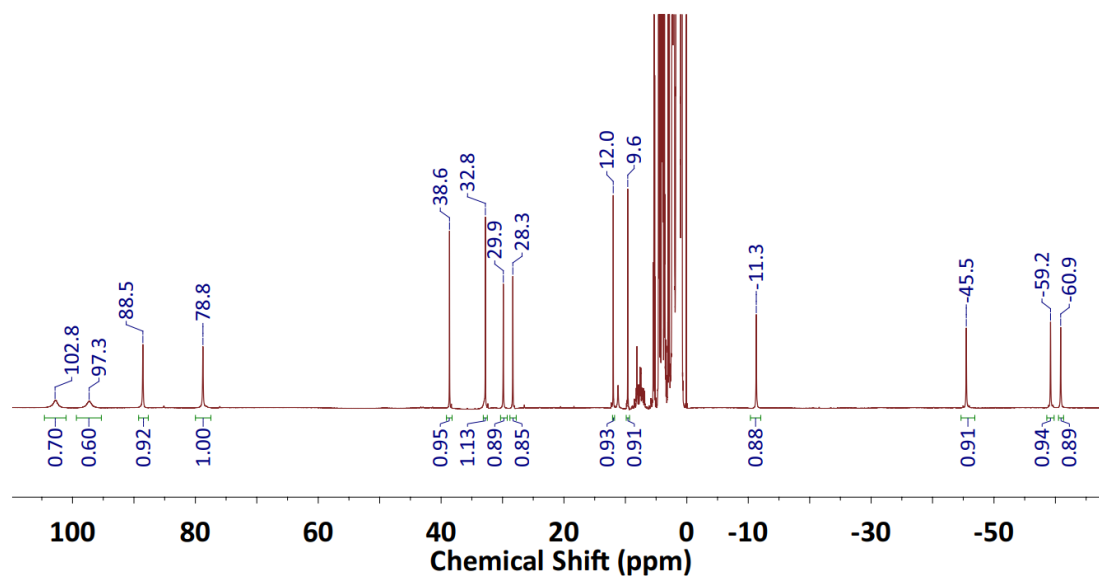


Fig. S1 Mass spectra of HMSC 1, top : experiment; bottom : simulation.

## 2. NMR measurements of HMSC **1**.

The  $^1\text{H}$  NMR spectra of **1** were recorded in  $[d_6]$ -DMSO with a Bruker AVIII HD 400 MHz spectrometer. We observed fourteen peaks which is consistent with the asymmetric structure of the metal complex.

In comparison with the results of our previous works of  $[\text{NiRu}_2(\mu_3\text{-dpa})_4\text{Cl}_2]$  and  $[\text{NiRu}_2\text{Ni}_2(\mu_5\text{-tpda})_4(\text{NCS})_2]$ ,<sup>1,2</sup> we can estimate the peak positions of the heterometallic chain and patterns. For a symmetric structure, the number of NMR peaks is reduced by one-half. Experimentally, we observed a total of 14 peaks in **1** (heptanuclear complex) which indicated a nonsymmetric complex. However, it is difficult to assign the peak positions because the metal ions are disordered in the crystal structure. However, we still can distinguish the number of NMR peaks between homonuclear and heteronuclear metal string complexes.



**Fig. S2** The  $^1\text{H}$  NMR spectrum of HMSC **1** in  $[d_6]$ -DMSO at 400 MHz.

### 3. Infrared spectra of HMSC 1.

The infrared spectra of **1** in KBr pellets were recorded on a Nicolet MAGNA-IR 550 type Fourier Transform IR spectrometer in the range of 500-4000  $\text{cm}^{-1}$ . The axial ligand  $\text{NCS}^-$  and  $\text{PF}_6^-$  anion peaks are detected at around 2069 and 836  $\text{cm}^{-1}$ , respectively.

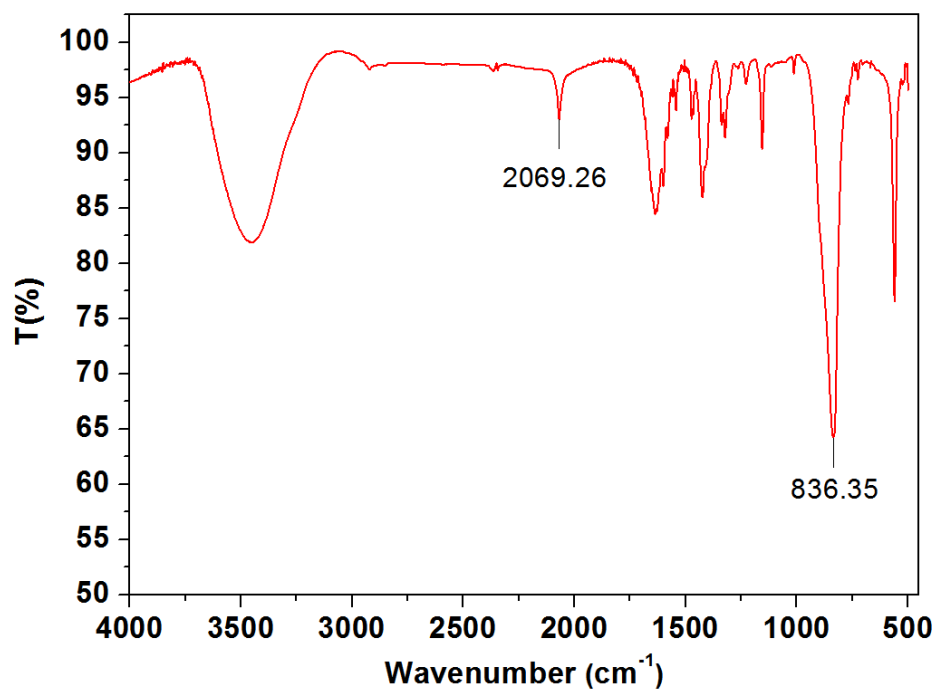


**Fig. S3** The IR spectra of HMSC **1**.

#### 4. Crystal structural data of HMSC 1.

**Table S1.** Crystal data for HMSC 1.

<b>1·2(CH<sub>2</sub>Cl<sub>2</sub>)(C<sub>3</sub>H<sub>7</sub>NO)</b>	
Identification code	ic19203
Empirical Formula	C <sub>86</sub> H <sub>64</sub> N <sub>30</sub> Ru <sub>2</sub> S <sub>2</sub> Cl <sub>8</sub> Ni <sub>5</sub> PF <sub>6</sub>
Formula weight	2506.05
Crystal color	dark-green
Crystal system	Monoclinic
Space group	C2/c
<i>a</i> [Å]	38.6072(15)
<i>b</i> [Å]	14.9578(6)
<i>c</i> [Å]	17.7771(8)
$\alpha$ [°]	90
$\beta$ [°]	115.2998(12)
$\gamma$ [°]	90
<i>V</i> [Å <sup>3</sup> ]	9281.2(7)
<i>Z</i>	4
<i>T</i> [K]	150(2)
$\rho_{\text{calcd}}$ [Mgm <sup>-3</sup> ]	1.793
<i>R1</i> <sup>[a]</sup> / <i>wR2</i> <sup>[b]</sup> [ <i>I</i> > 2σ( <i>I</i> )]	0.0422, 0.1032
<i>R1</i> <sup>[a]</sup> / <i>wR2</i> <sup>[b]</sup> (all data)	0.0649, 0.1305
GOF	1.095

[a]  $R1 = \sum |F_o| - |F_c| / \sum |F_o|$ . [b]  $wR2 = [\sum [w(F_o^2 - F_c^2)^2] / \sum [w(F_o^2)^2]]^{1/2}$ , in which  $w = 1 / \sigma^2(F_o^2) + (aP)^2 + bP$ ,  $P = (F_o^2 + 2F_c^2) / 3$ .

## 5. The EPR spectra and spectral simulation at 20 and 60 K.

We performed EPR measurements for complex **1** at 4, 20 and 60 K. The EPR spectra measured at 20 and 60 K are displayed in Fig. S4. The spectral peaks became broader when the temperatures raised. The peak at  $g_{\text{eff}} = 5.12$  became broadened at 60 K and merged with a peak at  $g_{\text{eff}} = 4.38$ . The other two much weaker peaks were no longer visible due to spectral broadening at higher temperatures. The spectral broadening is due to faster relaxation processes. This is consistent with the rapid increase of  $\chi_M$  value in the range of 4 - 30 K observed in magnetic susceptibility measurements. The best fit spectral parameters are given in Table S2. Note that the paramagnetic parameters remain the same but the linewidth and populations of each of the spin states are changing as a function of temperature.

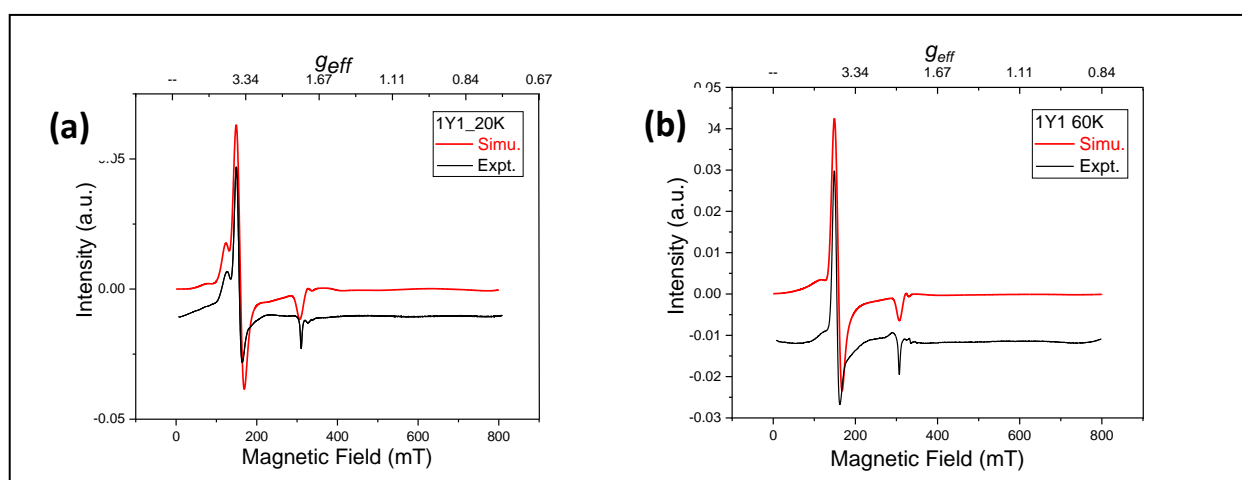


**Fig. S4** The experimental and simulated EPR spectra of complex **1** measured at (a) 20 K and (b) 60 K. The spectra were fitted with the EasySpin program in the MathLab platform. The spin Hamiltonian employed in the simulation is given as Eq. (2) in the manuscript.

**Table S2** Best fit paramagnetic parameters for complex **1** in DCM at 20 and 60K

Parameters*	$S_1 = 1/2$	$S_2 = 3/2$	$S_3 = 5/2$	$S_4 = 7/2$
$g$ -values	2.06, 2.09, 2.16	2.18	2.13	2.04
$D, E$ ( $\text{cm}^{-1}$ )	---	[30.2, -0.81]	[0.27, -0.033]	[0.27, -0.033]
Linewidth (mT) (20, 60 K)	15, 16	18, 20	30, 55	25, 55
Population (wt %) (20, 60 K)	2, 2	56, 51	23, 26	19, 21

\*The uncertainties in all of the fitting values are the same as those at 4K and are given in Table 2.

## References

1. G.-C. Huang, M. Bénard, M.-M. Rohmer, L.-A. Li, M.-J. Chiu, C.-Y. Yeh, G.-H. Lee, and S.-M. Peng, *Eur. J. Inorg. Chem.* 2008, 1767-1777.
2. M.-J. Huang, S.-A. Hua, M.-D. Fu, G.-C. Huang, C. Yin, C.-H. Ko, C.-K. Kuo, C.-H. Hsu, G.-H. Lee, K.-Y. Ho, C.-H. Wang, Y.-W. Yang, I.-C. Chen, S.-M. Peng and C.-h. Chen, *Chem.-Eur. J.* 2014, **20**, 4526-4531.